



HAL
open science

Effects of the cross-linking of the cellulosic fibrillar network on the macroscopic elastic behaviour of wood

Nhat-Tung Phan, François Auslender, Joseph Gril, Rostand Moutou Pitti

► To cite this version:

Nhat-Tung Phan, François Auslender, Joseph Gril, Rostand Moutou Pitti. Effects of the cross-linking of the cellulosic fibrillar network on the macroscopic elastic behaviour of wood. WCTE, Université de Oslo, Jun 2023, Oslo (Norway), Norway. pp.443-448, 10.52202/069179-0060 . hal-04366364v2

HAL Id: hal-04366364

<https://hal.science/hal-04366364v2>

Submitted on 29 Dec 2023

HAL is a multi-disciplinary open access archive for the deposit and dissemination of scientific research documents, whether they are published or not. The documents may come from teaching and research institutions in France or abroad, or from public or private research centers.

L'archive ouverte pluridisciplinaire **HAL**, est destinée au dépôt et à la diffusion de documents scientifiques de niveau recherche, publiés ou non, émanant des établissements d'enseignement et de recherche français ou étrangers, des laboratoires publics ou privés.

EFFECTS OF THE CROSS-LINKING OF THE CELLULOSIC FIBRILLAR NETWORK ON THE EFFECTIVE MACROSCOPIC BEHAVIOUR OF WOOD

Nhat-Tung Phan¹, François Auslender¹, Joseph Gril^{1,2}, Rostand Moutou Pitti^{1,3}

ABSTRACT: This study aims at analysing the influence of the fibrils oscillations and interconnexions on the macroscopic behaviour of wood. For that, a multi-scale model of softwood has been developed, with two options for the cell-wall level: a reference with no oscillations (0S) and oscillations and interconnexions in two directions (2S). The cell-wall and tissue effective behaviours are determined by using numerical homogenization for periodic media, while the succession of earlywood and latewood is dealt with analytically. It is observed that the influence of the fibrils oscillations is significant for some macroscopic moduli, such as the effective shear moduli \tilde{G}_{LT} and \tilde{G}_{LR} , while it isn't for other moduli at the macroscopic level. Furthermore, although the effect of the interconnexions is quite strong for some components of the elastic behaviour at the cell wall level, it would lose its significance at the macroscopic level, especially for low-density wood. This tendency can be explained by the interaction of layers from two neighbouring cells that compensate for the absence of interaction between fibrils in the 0S model. The effect becomes stronger in the case of a softened matrix.

KEYWORDS: macroscopic behaviour, hierarchical models, numerical homogenization, fibrils oscillations.

1 INTRODUCTION

Wood is one of the longest-standing and most universal materials used by humans. In response to environmental changes, population growth, and increasing standard of living, the global demand for lignocellulose material has accelerated [1]. The advantages of this material are mainly its availability and its excellent mechanical performance relative to the density, explained by its structural organization [2].

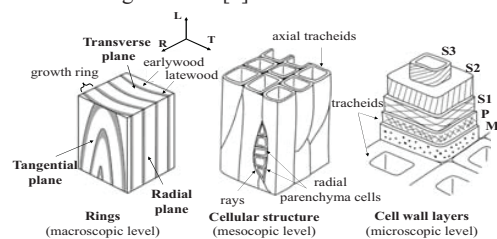


Figure 1: Hierarchical structure and anisotropy of a softwood

However, the study of wood has revealed a large variability of mechanical properties and various scales of heterogeneity. Thus, a better understanding of structure-property relationships is required to improve our capacity to design wood-derived products. Since wood is considered as a natural composite material with a complex multiscale organization, its behaviour is a consequence of

both the deformation mechanisms of its constituents and their spatial distribution at different scales. In this study, having in mind the case of a softwood, we will then describe wood at three main levels (see Figure 1): the macroscopic level - scale of the grown-rings, the mesoscopic level - scale of the tissues, and the microscopic level - scale of the cell walls.

This paper aims to investigate the influence of a more realistic cell wall morphology on the macroscopic behaviour of wood by considering curved and interconnected fibrils, rather than considering them parallel as classically in the literature [3, 4, 5]. To this end, we develop a multiscale model incorporating three different scales of wood microstructure as described above, ranging from cell walls to annual grown-rings, from which both numerical and analytical homogenization methods will be used to determine their effective behaviour by defining a periodic elementary cell at each scale considered.

2 METHODOLOGY

2.1 MULTI-SCALE MODEL

2.1.1 An anisotropic material at all scales: from the secondary wall to the growth-ring

The illustration of the hierarchical structure of the wood at different scales in Figure 1 highlights the preferred

¹Nhat-Tung Phan, François Auslender, Joseph Gril, Rostand Moutou Pitti, Université Clermont Auvergne, CNRS, Clermont Auvergne INP, Institut Pascal, F-63000 Clermont Ferrand, FRANCE nhat_tung.phan@uca.fr

²Joseph Gril, Université Clermont Auvergne, INRAE, Piaf, F-63000 Clermont Ferrand, FRANCE

³Rostand Moutou Pitti, IRT, Libreville Gabon

directions at each level. In this research, we make use of three orthonormal frames with in each case the first direction corresponding to the one with the most resistance and rigidity. They are represented in Figure 2 for the three considered levels. The three reference frames are: (L, R, T) for the growth-rings level, (1', 2', 3') for the tissues level and (1, 2, 3) for the cell walls level.

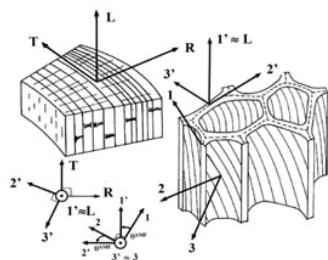


Figure 2: Macroscopic, mesoscopic and microscopic orientations [6].

2.1.2 Description of the wood microstructure at the 3 relevant scales

a) Wood cell wall microstructure

In the literature, the macrofibrils have classically been assumed to be straight and parallel to each other (Figure 3a). However, some experimental characterizations [7, 8] suggest that this is not the case and that the macrofibrils are curved and connected to each other [9]. These suggestions are similar to the models of an oscillating cellulose network originally proposed by Boyd [10], and later used by Gril [6].

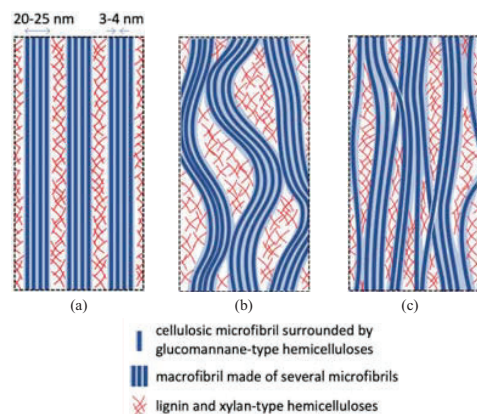


Figure 3: Interpretation of the interconnexions between macrofibrils: (a) classical representation with straight and parallel microfibrils; (b) Oscillations and lateral contacts between macrofibrils through hydrogen bonding; (c) connexions resulting from the random transfer of oscillating microfibrils between neighbouring macrofibrils [11].

Furthermore, this oscillating structure may be the reason for the puzzling orientation interpreted from tomography [12]. As to the nature of the links between macrofibrils, it can be speculated that macrofibrils oscillate by slight deviations from their main direction, and occasionally get into contact through hydrogen bonding with neighbouring

macrofibrils (Figure 3b). An alternative explanation is that some of the microfibrils composing a macrofibril could occasionally shift to the neighbouring one, resulting in stronger connections (Figure 3c). In any case, it seems reasonable to assume the existence of a network of macrofibrils laterally connected, separated by lignified matrix incrustations with more or less lenticular shapes, and both interpretations would be compatible with the subsequent modelling approach. For the sake of simplification, the macrofibrils will be simply be called fibrils in what follows.

From the schematic description of the secondary walls proposed by Boyd [10], we assume that the fibrils oscillate around a principal direction, that we name direction 1, corresponding to the one defined by the MFA (Figure 4a). Taking the case of perfectly aligned fibrils as a reference (Figure 4b), we will examine the effect of oscillated fibrils (Figure 4c). In this study, we will describe oscillations for which the fibrils can oscillate within both planes (1, 2) and (1, 3).

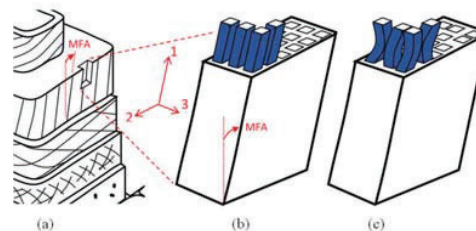


Figure 4: Representation of the material constituting the secondary cell wall: (a) position and orientation of a portion of the cell wall, (b) classical representation with straight and parallel fibrils and (c) improved description with oscillated and connected fibrils [11].

In order to analyse the influence of oscillated and connected fibrils on the effective behaviour of the cell wall, two periodic elementary cells that correspond to the 0S and 2S models, respectively, are meshed (Figure 5). The cell wall material is assumed to be the periodic repetition of each of the represented elementary cells.

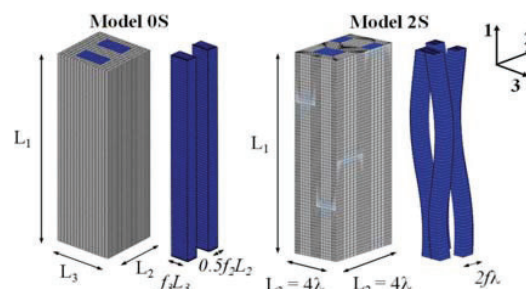


Figure 5: two different morphological models to describe the periodic elementary cell (Cast3M)

b) Cellular tissue microstructure

The tissue microstructure of wood is modelled on the basis of anatomical and morphological descriptions of the structure of wood at the tissue level, considering tissues composed only of longitudinal tracheids. We will thus neglect the parenchyma rays which are a minor component of softwood. The studied microstructure being

supposed to be periodic, we will consider a periodic unit cell to represent it and calculate its effective behaviour. Moreover, this elementary cell will be constructed by integrating additional assumptions, frequently used in the literature [13, 14, 15]:

- Invariance of the tissue structure in the longitudinal direction L, i.e. longitudinal irregularities at the points where the tracheids meet end to end are ignored;
- Invariance of the local density in the longitudinal direction.

Based on typical morphological parameters of softwoods at the tissue scale [16], earlywood (EW) and latewood (LW) are described as tissues consisting of a periodic arrangement of tissue microstructures of EW (Figure 6a) and LW (Figure 6b), respectively. Furthermore, each wall of the tissue microstructure consists of 3 layers (S1, S2, and S3), incorporating the primary wall and the middle lamella in the S1 layer.

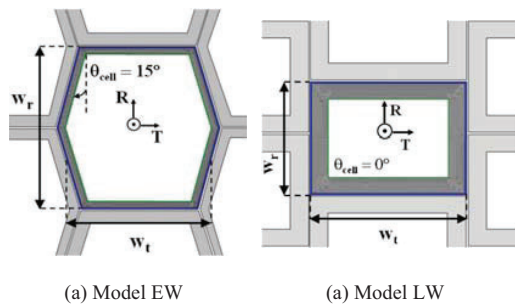


Figure 6: Geometric description of the two microstructures of EW and LW in the RT plane.

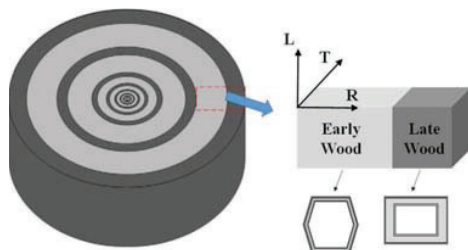


Figure 7: Schematically idealized model for the annual ring

c) Growth-ring microstructure

At the macroscopic scale, wood is described as a periodic arrangement of orthotropic homogeneous layers of EW and LW, without taking into account the curvature of the rings (see Figure 7). Although in reality the transition between EW and LW is gradual, the choice of a ring consisting of two layers has been made in order to achieve an equivalent effect in terms of contribution to transverse anisotropy.

2.2 CALCULATION OF THE EFFECTIVE BEHAVIOUR

On the one hand, we determine the effective elastic behaviour at both the cell wall and tissue scales by using a numerical homogenization procedure for its periodic microstructures in the first two steps of the developed

multiscale model. On the other hand, the macroscopic elastic properties of the wood corresponding to the succession model of EW and LW are determined analytically and correspond to the last step of the multiscale model. Furthermore, the interaction of the material parameters between the different levels of the multiscale model are also taken into account.

2.2.1 Local problem

For determining the effective elastic properties of the different periodic microstructures, we make use of a deformation approach and apply to each periodic unit cell periodic boundary conditions of the type $\underline{u}(x) = \underline{\bar{\varepsilon}}x + \underline{u}'(x)$ where $\underline{\bar{\varepsilon}}$ is the imposed macroscopic strain and $\underline{u}'(x)$ a periodic displacement field [17]. The local problem to be solved reads as follows:

$$\left\{ \begin{array}{l} \text{div}(\underline{\sigma}(x)) = 0 \\ \underline{\sigma}(x) = \underline{\underline{C}}(x) : \underline{\varepsilon}(x) \\ \underline{\varepsilon}(x) = \frac{1}{2} \left(\frac{\partial \underline{u}(x)}{\partial (x)} + \frac{\partial \underline{u}(x)}{\partial (x)}^T \right) \\ \underline{u}(x) = \underline{\bar{\varepsilon}}x + \underline{u}'(x), \text{ with periodic } \underline{u}', \forall x \in \partial\Omega \end{array} \right\} \forall x \in \Omega \quad (1)$$

where Ω stands for the RVE, i.e. the periodic unit cell, and $\partial\Omega$ the cell boundary. The fourth-order tensor $\underline{\underline{C}}(x)$ is given by:

$$\underline{\underline{C}}(x) = \sum_{r=M,F} \underline{\underline{C}}^r \cdot \chi^r(x) = \underline{\underline{C}}^M \cdot \chi^M(x) + \underline{\underline{C}}^F \cdot \chi^F(x)$$

where $\chi^r(x)$ is the characteristic function of the phase r , equal to 1 if x belongs to the phase r and zero otherwise. The tensors $\underline{\underline{C}}^r$ are the tensors of the elastic moduli of the phases r .

2.2.2 Numerical homogenization

To calculate the effective behaviour of a periodic elementary cell corresponding to the cell wall (Figure 5) and tissue (Figure 6) microstructures, we make use of a deformation approach and apply periodic boundary conditions (PBC).

By applying 6 different elementary loadings to the periodic unit cell and solving by means of the FE method the local problem, we obtain for each elementary loading the local stress field, thus allowing us to determine the macroscopic stress which is classically defined by:

$$\underline{\underline{\bar{\sigma}}} = \langle \underline{\underline{\sigma}} \rangle = \frac{1}{|\text{VER}|} \int_{\text{VER}} \underline{\underline{\sigma}}(x) dx \quad (2)$$

The tensor of the effective elastic moduli $\underline{\underline{\tilde{C}}}$ of the cell wall is then obtained by the following relation

$$\underline{\underline{\bar{\sigma}}} = \underline{\underline{\tilde{C}}} : \underline{\underline{\bar{\varepsilon}}} \quad (3)$$

which, by using Voigt notations, can be rewritten as

$$\begin{pmatrix} \bar{\sigma}_1 \\ \bar{\sigma}_2 \\ \bar{\sigma}_3 \\ \bar{\sigma}_4 \\ \bar{\sigma}_5 \\ \bar{\sigma}_6 \end{pmatrix} = \begin{pmatrix} \tilde{C}_{11} & \tilde{C}_{12} & \tilde{C}_{13} & \tilde{C}_{14} & \tilde{C}_{15} & \tilde{C}_{16} \\ \tilde{C}_{21} & \tilde{C}_{22} & \tilde{C}_{23} & \tilde{C}_{24} & \tilde{C}_{25} & \tilde{C}_{26} \\ \tilde{C}_{31} & \tilde{C}_{32} & \tilde{C}_{33} & \tilde{C}_{34} & \tilde{C}_{35} & \tilde{C}_{36} \\ \tilde{C}_{41} & \tilde{C}_{42} & \tilde{C}_{43} & \tilde{C}_{44} & \tilde{C}_{45} & \tilde{C}_{46} \\ \tilde{C}_{51} & \tilde{C}_{52} & \tilde{C}_{53} & \tilde{C}_{54} & \tilde{C}_{55} & \tilde{C}_{56} \\ \tilde{C}_{61} & \tilde{C}_{62} & \tilde{C}_{63} & \tilde{C}_{64} & \tilde{C}_{65} & \tilde{C}_{66} \end{pmatrix} \begin{pmatrix} \bar{\varepsilon}_1 \\ \bar{\varepsilon}_2 \\ \bar{\varepsilon}_3 \\ \bar{\varepsilon}_4 \\ \bar{\varepsilon}_5 \\ \bar{\varepsilon}_6 \end{pmatrix} \quad (4)$$

where $\bar{\sigma}_i = \bar{\sigma}_{ii}$, $\bar{\epsilon}_i = \bar{\epsilon}_{ii}$ for $i = 1$ to 3 and $\bar{\sigma}_4 = \bar{\sigma}_{23}$; $\bar{\sigma}_5 = \bar{\sigma}_{13}$; $\bar{\sigma}_6 = \bar{\sigma}_{12}$ and $\bar{\epsilon}_4 = 2\bar{\epsilon}_{23}$; $\bar{\epsilon}_5 = 2\bar{\epsilon}_{13}$; $\bar{\epsilon}_6 = 2\bar{\epsilon}_{12}$.

For instance, if we apply an elementary loading of the form $\underline{\underline{\epsilon}} = \underline{e}_1 \otimes \underline{e}_1$, the first column of the second-order tensor $\underline{\underline{\tilde{C}}}$ is given by:

$$\tilde{C}_{11} = \bar{\sigma}_1 = \langle \sigma_{11} \rangle; \tilde{C}_{21} = \bar{\sigma}_2 = \langle \sigma_{22} \rangle; \tilde{C}_{31} = \bar{\sigma}_3 = \langle \sigma_{33} \rangle; \tilde{C}_{41} = \bar{\sigma}_4 = \langle \sigma_{23} \rangle; \tilde{C}_{51} = \bar{\sigma}_5 = \langle \sigma_{13} \rangle; \tilde{C}_{61} = \bar{\sigma}_6 = \langle \sigma_{12} \rangle.$$

Accordingly, the application of 6 independent elementary loadings provide the whole effective tensor $\underline{\underline{\tilde{C}}}$ of elastic moduli.

Moreover, by symmetry arguments related to the geometry of the elementary cell and the phase behaviour, it is shown that the effective behaviour of both the cell wall and tissue is necessarily orthotropic.

2.2.3 Analytical homogenization

The macroscopic behaviour of wood in the (L, R, T) directions is calculated by using an analytical solution for a bi-laminate consisting of the periodic repetition of two orthotropic elastic layers of earlywood and latewood (see Figure 7).

3 RESULTS AND DISCUSSION

In this work, we make use of the above-mentioned multiscale approach was used in this research to study the relationships between wood microstructure and its elastic properties. More specifically, this work aims to analyse through parametric studies the influence of oscillated and interconnected fibrils within the cell wall on the elastic effective properties of wood at three different scales.

3.1 THE CELL WALL LEVEL

The parametric studies are performed for both microstructure models (OS) and (2S) of the cell wall by varying different geometrical parameters such as the shape ratio $r_\phi = L_1/L_2$, the fibril volume fraction c , the ratio of lamellar matrix on lenticular matrix $r_\lambda = V_{\text{lamellar matrix}}/V_{\text{lenticular matrix}}$ and material parameter (phase contrast: ratio E_L^F/E^M where E_L^F is the longitudinal Young's modulus of the fibrils and E^M is the Young's modulus of the matrix). Three effects associated with the fibrils oscillations are highlighted: those induced by the orientation of the fibrils, by the contact between the fibrils, and finally by the heterogeneous spatial distribution of the matrix between the oscillating fibrils (see Figure 8).

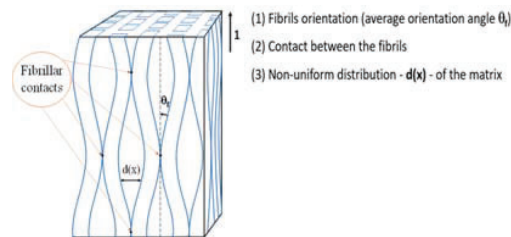


Figure 8: Illustration of the 3 effects induced by the undulations of the fibrils.

Furthermore, it is observed that the 2S model have a significant impact on the effective coefficients \tilde{C}_{12} , \tilde{C}_{66} and \tilde{C}_{13} , \tilde{C}_{55} which are significantly influenced by the fibril oscillations in the (1, 2) plane and (1, 3) plane, respectively. Besides, the 2S model is able to take into account the influence of oscillated fibrils in the (2, 3) plane by the observations associated with the effective coefficients et \tilde{C}_{23} , \tilde{C}_{44} , respectively.

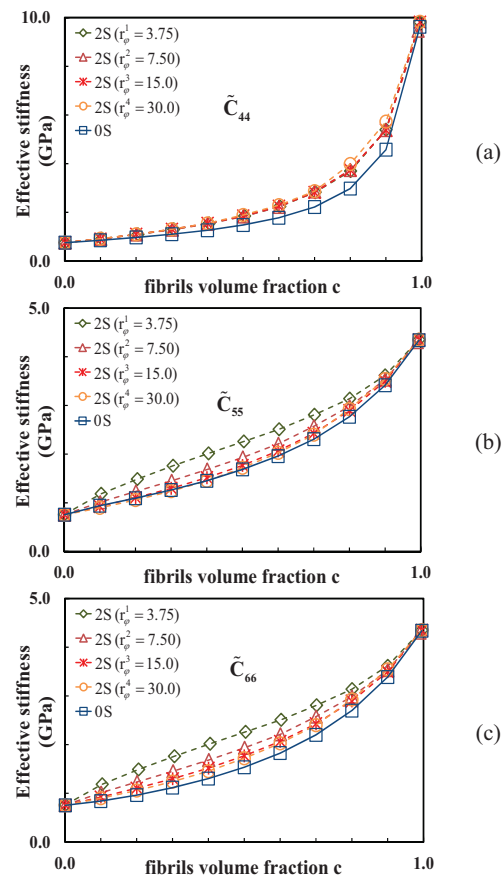


Figure 9: Variations of the effective moduli \tilde{C}_{ij} as functions of the volume fraction ($r_\lambda = 1$)

3.2 THE TISSUE LEVEL

Following the observations carried out at the cell wall level, we have shown at the tissue scale that the influence of the oscillated and interconnected fibrils increases with the relative density of the tissue. However, although the effects induced by the fibril oscillations are quite strong for some components of elastic behaviour at the cell wall scale, it loses its importance at the tissue level, especially for low density wood. This trend can be explained by the antisymmetric sloping of microfibrils in adjacent cell walls. Thus, for denser wood where the interaction between adjacent cell walls is less dominant, the effect of fibril oscillations remains significant. To highlight these results, we present in Figure 10 the evolutions of the 3

effective shear moduli \tilde{G}_{ij} as a function of relative density (wood density divided by cell-wall density) for the latewood case.

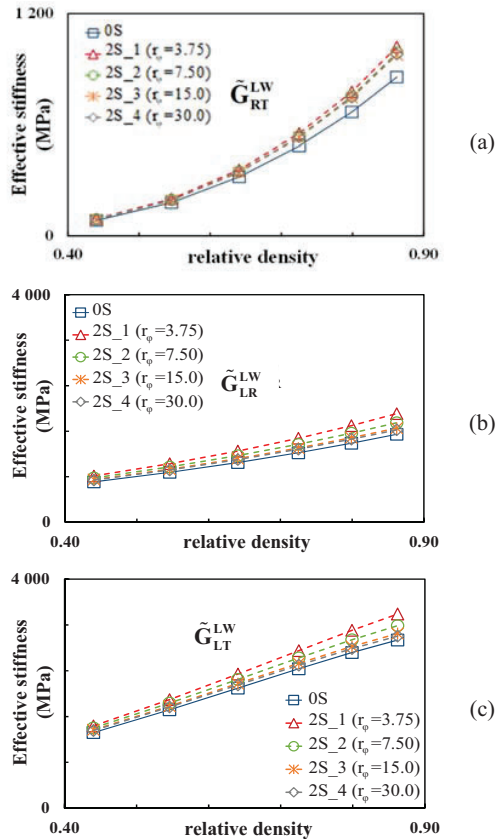
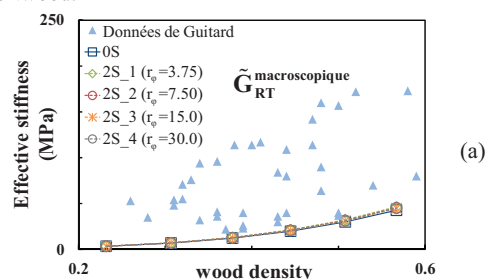


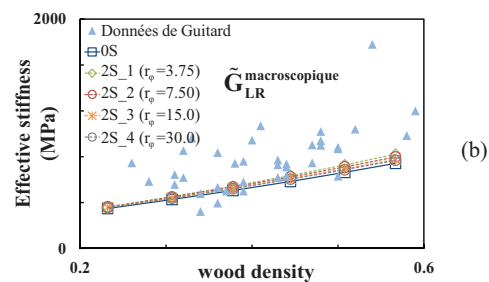
Figure 10: Evolution of the effective \tilde{G}_{ij} components as a function of relative density for the LW model with the different data associated with the OS and 2S models

3.3 THE GROWN-RING LEVEL

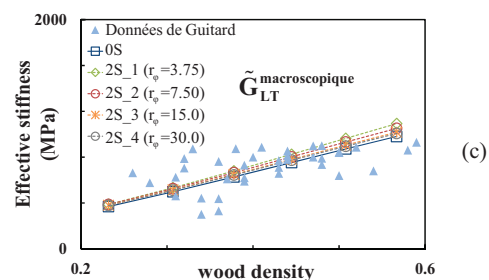
Based on Figure 11, the study of the influence of fibril oscillations on the macroscopic behaviour of wood via the presented multiscale model shows that the results obtained are similar to those observed at the grown-ring level. In addition, we also present for comparison purposes the experimental data of Guitard [18] for softwood.



(a)



(b)



(c)

Figure 11: Evolution of the effective moduli \tilde{G}_{ij} as a function of wood density for the two microstructures OS and 2S

4 CONCLUSION AND PERSPECTIVES

Using the presented multiscale model, we showed that the influence of the oscillated and interconnected fibrils is significant for some macroscopic moduli, such as effective shear moduli, while it is not significant for other moduli at the macroscopic level (grown-ring scale). Furthermore, the proposed multiscale model provides macroscopic elastic properties and their evolutions as a function of wood density which are close to those observed experimentally for softwoods, with the exception of the modulus \tilde{G}_{RT} which is strongly underestimated. Lastly, although the effect of fibril crosslinks is quite strong for some components of the elastic behaviour at the cell wall level, it loses its importance at the macroscopic level, especially for low-density wood.

In order to study the influence of fibril oscillations not only on the effective elastic properties of wood at the three scales considered, an extension of the presented procedure to the case of linear hygro-elastic behaviour, has been developed within the multiscale model. It is based on FE calculations associated with the linear thermo-elasticity model, has been developed within the multi-scale model. This procedure allows to take into account the deformations induced in the absence of mechanical loading by an increase (respectively a decrease) of the water content which leads to a swelling (respectively a shrinking) of the wood.

REFERENCES

- [1] Hansen, E., Juslin, H., 2018. Strategic Marketing in the Global Forest Industries, Oregon State University. Ed.
- [2] Salmén, L., 2018. Wood Cell Wall Structure and Organisation in Relation to Mechanics. Springer International Publishing AG.
- [3] Harrington, J.J., 2002. Hierarchical modelling of softwood hygro-elastic properties. University of Canterbury, Christchurch, New Zealand.
- [4] Persson, K., 2000. Micromechanical modelling of wood and fibre properties (Structural Mechanics). Lund University, Sweden.
- [5] Rafsanjani, A.A., 2013. Multiscale poroelastic model - Bridging the gap from cellular to macroscopic scale (Doctor of Sciences). ETH Zurich.
- [6] Gril, J., 1988. Une modelisation du comportement hygro-rheologique du bois a partir de sa microstructure. Paris 6.
- [7] Bardage, S., Donaldson, L., Tokoh, C., Daniel, G., 2004. Ultrastructure of the cell wall of unbeaten Norwayspruce pulp fibre surfaces. Nordic Pulp & Paper Research Journal 19, 448–452.
- [8] Salmén, L., Stevanic, J.S., Holmqvist, C. and Yu, S., 2021. Moisture induced straining of the cellulosic microfibril. Cellulose, 28(6), pp.3347-3357.
- [9] Salmén, L. and Burgert, I., 2009. Cell wall features with regard to mechanical performance. A review COST Action E35 2004–2008: Wood machining–micromechanics and fracture.
- [10] Boyd, J.D., 1982. An anatomical explanation for visco-elastic and mechano-sorptive creep in wood, and effects of loading rate on strength. New Perspectives in Wood Anatomy 171–222.
- [11] Phan NT., Auslender F., Gril J., Moutou Pitti R.. Influence of the cross-linking of the cellulosic fibrillar network on the effective hygro-mechanical behavior of the wood cell wall. Acta Mechanica. 2022.
- [12] Reza, M., Ruokolainen, J., Vourinen, T., 2014. Out-of-plane orientation of cellulose elementary fibrils on spruce tracheid wall based on imaging with high-resolution transmission electron microscopy. Planta 240, 565–573.
- [13] Astley, R.J., Stol, K.A., Harrington, J.J., 1998. Modelling the elastic properties of softwood. Part II: The cellular microstructure. Holz Als Roh- Werkst. Vol. 56, 43–50.
- [14] Koponen, S., Toratti, T., Kanerva, P., 1991. Modelling elastic and shrinkage properties of wood based on cell structure. Wood Sci. Technol. 25, 25–32.
- [15] Mishnaevsky Jr, L., Qing, H., 2008. Micromechanical modelling of mechanical behaviour and strength of wood: State-of-the-art review. Comput. Mater. Sci. 44, 363–370.
- [16] Fengel, D., 1969. The ultrastructure of cellulose from wood Part 1: Wood as the basic material for the isolation of cellulose. Wood Science and Technology 3, 203–217.
- [17] Bornert, M., Bretheau, T., Gilormini, P., 2001. Homogénéisation en mécanique des matériaux 1: matériaux aléatoires élastiques et milieux périodiques, Mécanique et Ingénierie des Matériaux.
- [18] Guitard, D., 1987. Mécanique du matériau bois et composites, Cépaduès. ed.